

Kinetics and Molecular Weight Control of the Polymerization of Acrylamide via RAFT[†]

David B. Thomas,^{*} Anthony J. Convertine,[‡] Leslie J. Myrick,[‡] Charles W. Scales,[‡] Adam E. Smith,[‡] Andrew B. Lowe,[§] Yulia A. Vasilieva,[‡] Neil Ayres,[‡] and Charles L. McCormick^{*,‡,§}

Department of Polymer Science, University of Southern Mississippi, Hattiesburg, Mississippi 39406-0076, and Department of Chemistry and Biochemistry, University of Southern Mississippi, Hattiesburg, Mississippi 39406-5043

Received October 17, 2003; Revised Manuscript Received September 2, 2004

ABSTRACT: The reversible addition–fragmentation chain transfer (RAFT) polymerization of acrylamide (AM) was studied in order to establish reaction conditions which would provide optimal rates of monomer conversion and to determine reasons for deviation of theoretical and experimental molecular weights, the former predicted from current models. To this end, chain transfer agents (CTAs) and initiators were selected and experiments performed in water and in dimethyl sulfoxide (DMSO) at specified CTA/initiator ratios and temperatures. Higher apparent rates of polymerization were achieved utilizing CTAs with higher intermediate fragmentation rates, larger initiator concentrations, and higher temperatures. For RAFT polymerization of acrylamide under these experimental conditions, a continuing supply of radicals was required in order to achieve reasonable conversions. The deviations of experimentally measured molecular weights from those theoretically predicted are a function of the CTA utilized and parallel the extent of rate retardation. The deviations are, at least in part, consistent with significant early radical coupling of stable intermediate species during the preequilibrium period (or the recently proposed CTA “initialization” period). These effects are apparent in both aqueous buffer and DMSO. The retardation effects and eventual loss of linearity of the first-order kinetic plots at extended times are also consistent with termination processes although these experiments alone do not rule out alternative mechanisms of reversible termination or slow fragmentation of intermediate species. For RAFT polymerizations in DMSO mediated by the trithiocarbonate CTA, reaction rates are significantly faster, and near quantitative conversions can be reached with proper initiator choice.

Introduction

Polymers with predictable molecular weights, narrow molecular weight distributions, and controlled architectures (block copolymers, star polymers, etc.) continue to be of considerable interest in research laboratories since they are excellent model systems for establishing structure–property–performance relationships. Traditional synthetic routes to such polymers, including anionic, cationic, and group transfer polymerizations, require stringent control over reagent purity and reaction conditions. In recent years, however, controlled radical polymerization techniques,¹ including atom transfer radical polymerization,^{2,3} nitroxide-mediated polymerization,^{4,5} and reversible addition–fragmentation chain transfer (RAFT) polymerization,^{6–8} have shown great promise as robust routes for advanced macromolecular synthesis. In our hands the RAFT process has proved to be particularly versatile in terms of reaction conditions and monomer selection.

Our earliest RAFT polymerizations utilized both cationic and anionic styrenic monomers for formation of pH-responsive diblock copolymers.⁹ More recently, we have focused on the controlled polymerization of industrially important acrylamido monomers,¹⁰ including anionic,^{11,12} cationic,¹³ zwitterionic,^{14,15} and neutral derivatives.^{16–18,19} In these studies, we found the RAFT

process to be very well suited to the controlled polymerization of N-substituted and N,N-disubstituted acrylamido monomers in both organic^{17,19} and aqueous media.^{11,15,16,20}

In an initial communication,¹⁸ we reported the controlled RAFT homopolymerization of acrylamide in an aqueous environment and subsequent chain extension of the macro chain transfer agent (macroCTA). Most significantly, moderately acidic conditions were necessary to avoid hydrolytic loss of thiocarbonylthio end groups and thus allow the successful controlled polymerization of acrylamide in water. Subsequently, we determined rate constants for hydrolysis and aminolysis of a representative chain transfer agent and two macroCTAs at selected pH values.²¹ On the basis of these rate constants, mathematical relationships were then developed to predict the number of living chain ends and molecular weights at specific conversions. Experimental molecular weights from SEC/MALLS analysis of polyacrylamide and poly(2-acrylamido-2-methyl propanesulfonate) prepared using CTA **3** (Figure 1) were in reasonable agreement with our hydrolysis/aminolysis-modified predictions.

However, there were unresolved issues in these aqueous polymerizations of acrylamide mediated by dithioesters. Though showing linear growth of molecular weight with conversion, the disparity between predicted and theoretical molecular weights remained considerable, despite utilizing conditions virtually eliminating aminolysis and greatly limiting hydrolysis of the CTA. Also, the slow rate of acrylamide polymerization under these conditions limited conversion to <28%.

[†] Paper Number 109 in a series entitled “Water-Soluble Polymers”.

[‡] Department of Polymer Science.

[§] Department of Chemistry and Biochemistry.

^{*} To whom correspondence should be addressed.

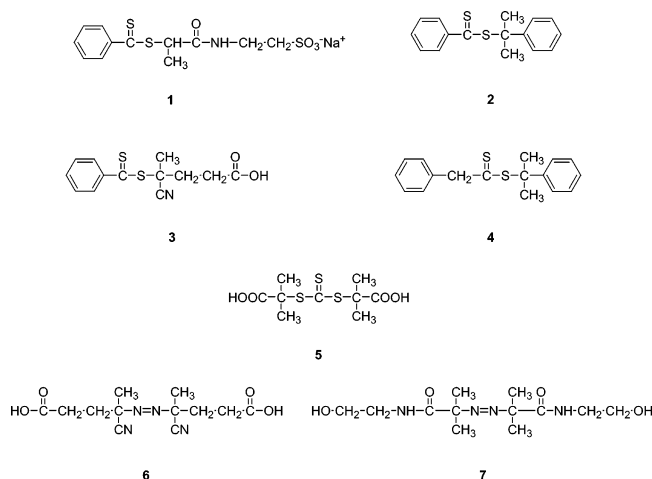


Figure 1. Chain transfer agents: sodium 2-(2-thiobenzoylsulfonylpropionylamino)ethanesulfonate (**1**), cumyl dithiobenzoate (**2**), 4-cyanopentanoic acid dithiobenzoate (**3**), cumylphenyldithioacetate (**4**), and 2-(1-carboxy-1-methyl-ethylsulfanyltiocarbonylsulfanyl)-2-methylpropionic acid (**5**) and initiators 4,4'-azobis(4-cyanovaleic acid) (**6**) and 2,2'-azobis[2-methyl-N-(2-hydroxyethyl)propionamide] (**7**) employed in the RAFT polymerization of acrylamide.

In earlier work, we measured molecular weight values 30–50% higher than those predicted by theory and observed severe rate retardation in dithioester-mediated polymerizations of *N,N*-dimethylacrylamide.¹⁶ Similar observations have been reported for the polymerization of *N*-acryloylmorpholine.²² Most recently, we have measured molecular weights for zwitterionic¹⁵ and cationic methacrylamido¹³ polymers to be significantly larger than those theoretically predicted. In these latest cases, the molecular weights were determined directly by SEC/MALLS rather than by comparison with GPC standards. Therefore, we concluded mechanisms other than hydrolysis/aminolysis were operative, at least in acrylamido monomer polymerization.

In this paper we report (a) RAFT conditions for attaining higher rates of polymerization and higher conversion while maintaining macroCTA functionality and (b) possible reasons for the experimentally measured molecular weight “overshoot” observed for acrylamido systems. Herein we examine factors affecting both kinetics and control of molecular weight and polydispersity of acrylamide polymerization in the organic solvent dimethyl sulfoxide (DMSO) considering initiator, CTA, and temperature.

Experimental Section

Materials. All chemicals were purchased from Fisher or Aldrich at the highest available purity and used as received unless otherwise noted. 2,2'-Azobis[2-methyl-N-(2-hydroxyethyl)propionamide] and 4,4'-azobis(4-cyanovaleic acid) (gifts from Wako Chemicals USA Inc.) were recrystallized from dioxane and methanol, respectively. Sodium dithiobenzoate,⁹ cumyl dithiobenzoate,²³ 4-cyanopentanoic acid dithiobenzoate (**3**),⁹ cumylphenyl dithioacetate (**4**),^{23,24} and 2-(1-carboxy-1-methylethylsulfanyltiocarbonylsulfanyl)-2-methylpropionic acid (**5**)²⁵ were prepared according to previously reported procedures. Acrylamide was recrystallized three times from acetone. *N,N*-Dimethylacrylamide (DMA) was vacuum-distilled immediately prior to use.

Sodium 2-(2-Thiobenzoylsulfonylpropionylamino)ethanesulfonate (1**)** (Figure 1).²⁶ Sodium 2-(2-bromopropionylamino)ethanesulfonate was prepared by first dissolving 2-aminoethanesulfonic acid (25.6 g, 205 mmol) and NaOH (16.4 g, 410 mmol) in deionized water (20 mL). 2-Bromopro-

pionyl bromide (44.0 g, 204 mmol) dissolved in dichloromethane (50 mL) was then added dropwise at 0 °C over 30 min. During the addition, a large quantity of solid was produced, requiring occasional manual mixing. After 1 h at ambient temperature, the mixture was filtered and the solid washed with a small amount of absolute ethanol (~10 mL) followed by diethyl ether (~50 mL) and then dried in vacuo. Compound **1** was prepared by dissolving freshly synthesized sodium dithiobenzoate (9.12 g) in 1 mL of water, to which sodium 2-(2-bromopropionylamino)ethanesulfonate (8.5 g dissolved in 6 mL of water) was added. Immediately upon mixing, a precipitate formed accompanied by a strong exotherm. After 24 h at room temperature, the solid was filtered and washed with 2 mL of water. The filtrate was precipitated in acetone, yielding a pink powder that was isolated by centrifugation. The precipitate was washed with acetone and dissolved in water, and acetone was added to the point of incipient precipitation. Dark red needles (mp 215–218 °C) were obtained by cooling this solution at 4 °C for an extended period. ¹H NMR: δ = 1.22, 1.45 (2d, 3H), 2.92 (d, 3H), 3.44 (d, 3H), 4.35 (q, 1H), 7.29 (q, 2H), 7.44 (d, 1H), 7.76 (d, 2H). ¹³C NMR: 15.77, 35.55, 49.59, 50.08, 126.81 (CH), 128.82 (CH), 133.39 (CH), 144.30 (C), 173.71 (C=O), 228.95 (C=S). Crystals contained 1.68 wt % water. Analysis for CNS Calculated: C, 38.0%; N, 3.69%; S, 25.3%. Found: C, 37.9%; N, 3.58%; S, 25.3%. IR (cm⁻¹): 3438 (m), 1648 (s), 1554 (m), 1210 (s), 1037 (s). UV-vis: ϵ (483 nm) = 135 L mol⁻¹ cm⁻¹.

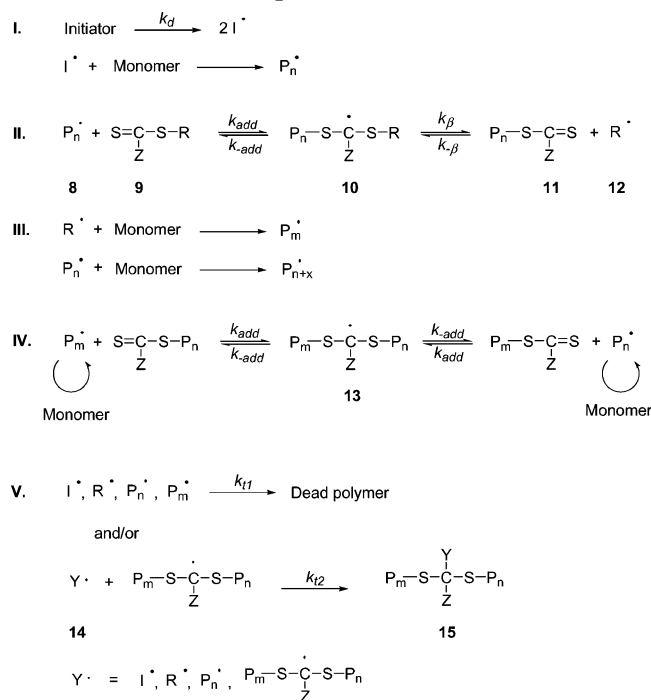
General RAFT Polymerization Procedure. All polymerizations were carried out at a 2.0 M monomer concentration in individual, septa-sealed vials that were purged with nitrogen for at least 20 min prior to reaction. The monomer to CTA ratio $[\text{M}]/[\text{CTA}]_0$ was held constant at 800/1 while the initial CTA-to-initiator ratio ($[\text{CTA}]_0/[\text{I}]_0$) was varied in order to assess control of conversion and molecular weight. Aqueous polymerizations were carried out in buffer solutions (pH = 5.0) containing 0.272 M acetic acid and 0.728 M sodium acetate with **1** as the CTA and **7** as the initiator. Polymerizations in DMSO were performed with **2**, **3**, **4**, or **5** as the CTA and **6** or **7** as the initiator.

MacroCTA of Acrylamide. Acrylamide (15.4 g, 0.217 mol), 2-(1-carboxy-1-methylethylsulfanyltiocarbonylsulfanyl)-2-methylpropionic acid (76.6 mg, 0.271 mmol), and V-501 (15.2 mg, 0.0542 mmol) were added to a 250 mL, round-bottom flask equipped with a magnetic stirring bar. Dimethyl sulfoxide was added until the total solution volume was 108.5 mL. The flask was sealed with a rubber septum, and the contents were purged with nitrogen for 60 min. The flask was subsequently immersed in a water bath preheated to 70 °C, and the polymerization was allowed to proceed for 4 h before being quenched by rapid cooling with liquid nitrogen. MacroCTA AM₅ was then purified by direct precipitation into a 20 times excess of acetone.

Synthesis of Poly(AM-*b*-DMA-*b*-AM). Dimethylacrylamide (10.0 g, 0.101 mol), macroCTA AM₅ (36 200 g/mol, PDI = 1.25) (4.56 g, 0.126 mmol), and V-501 (7.07 mg, 0.025 mmol) were added to a 100 mL, round-bottom flask equipped with a magnetic stirring bar. Aqueous acetate buffer solution (pH = 5.0) was added until the total solution volume was 50.4 mL. The flask was sealed with a rubber septum, and the contents were purged with nitrogen for 60 min. The flask was subsequently immersed in a water bath at 70 °C, and the polymerization was allowed to proceed for 4 h before being quenched with by immersion in liquid nitrogen. The resulting solution was purified by dialysis against deionized water, and the block copolymer was isolated by lyophilization.

Block copolymer composition was determined using ¹H NMR spectroscopy by a comparison of peaks associated with the two comonomers. The first signal, I₁ (1.21–1.96 ppm), is comprised of the methylene protons of the acrylamide and DMA residues (2H/mol AM + 2H/mol DMA), and the second signal, I₂ (1.99–3.32 ppm), is comprised of the methyne protons of each monomer residue plus the methyl protons from DMA (7 H/mol DMA + 1 H/mol AM). The mole fraction of DMA residues, X_{DMA} , was then calculated according to the equation $X_{\text{DMA}} = (2(I_2) - I_1)/(6(I_1))$.

Scheme 1. Proposed RAFT Mechanism



Instrumentation. Polymerization mixtures were analyzed directly by aqueous size exclusion chromatography (ASEC), using an eluent of 20% acetonitrile/80% 0.05 M $\text{Na}_2\text{SO}_4(\text{aq})$ and a flow rate of 0.5 mL/min at 25 °C, Viscotek TSK Viscogel columns (G3000 PW_{XL} (<50 000 g/mol, 200 Å) and G4000 PW_{XL} (2000–300 000 g/mol, 500 Å)), with a Polymer Labs LC 1200 UV/vis, Wyatt Optilab DSP interferometric refractometer, and Wyatt DAWN EOS multiangle laser light scattering detectors (690 nm). Conversions were determined by comparing the area of the UV signal at 633 nm corresponding to monomer at $t = 0$ to the area at t_x . The dn/dc of polyacrylamide in the above eluent was previously determined to be 0.160 mL/g at 25 °C.²⁷ Absolute molecular weights and polydispersities were calculated using the Wyatt ASTRA SEC/LS software package. IR spectra were recorded with a Nicolet Protégé 460 spectrometer. CHNS elemental microanalysis was performed by Quantitative Technologies, Inc., in Whitehouse, NJ.

Design Criteria and Results

According to the currently proposed mechanism, control in RAFT-mediated polymerizations is achieved through the rapid degenerative transfer of a thiocarbonylthio species (Scheme 1).^{8,31} When a propagating radical (8) adds to such a transfer agent (9), an intermediate radical species (10) is formed (II, Scheme 1). This intermediate may then fragment to produce a new radical, R^\bullet (12), which in turn initiates a new chain involved in establishing the main equilibrium (IV, Scheme 1).

The theoretical molecular weight, $M_{n,\text{th}}$, at conversion ρ may be predicted by eq 1

$$M_{n,\text{th}} = \frac{M_{\text{MW}}[\text{M}]_0\rho}{[\text{CTA}]_0 + 2f[\text{I}]_0(1 - e^{-k_d t})} + \text{CTA}_{\text{MW}} \quad (1)$$

in which M_{MW} and CTA_{MW} are the formula weights of monomer and CTA; $[\text{CTA}]_0$ and $[\text{M}]_0$ are the initial CTA and monomer concentrations. The right-hand side of the denominator accounts for radicals derived from initiator with an initial concentration $[\text{I}]_0$ at time t with a

decomposition rate, k_d . The initiator efficiency is represented by f . In an ideal RAFT process, polymer directly derived from the initiators is thought to be minimal, and thus the second term in the denominator becomes negligible.

Aqueous RAFT Polymerizations of Acrylamide.

CTA 1 was designed and synthesized in our laboratories to act as a versatile agent for the RAFT polymerization of a variety of monomers in aqueous media. This dithioester, prepared by a two-step procedure outlined in the Experimental Section, possesses a sulfonate functionality allowing CTA-mediated polymerization across a wide pH range. The secondary amide leaving group was incorporated to closely match that of the propagating chain end of acrylamido polymers. We have previously employed this strategy to minimize polydispersity and to reduce or eliminate the initial induction period.¹⁷

We have demonstrated that it is possible to significantly reduce CTA degradation during polymerization arising from nucleophilic attack of water and/or ammonia, the latter a product of acrylamide monomer or polymer hydrolysis.²¹ However, even under optimal conditions (i.e., lowering the pH to 5.0 and conducting the polymerization at 70 °C), the apparent rate of monomer conversion remains within 1 order of magnitude of the rate for hydrolysis of the macroCTA end group. Therefore, it is essential to accomplish the polymerization in the shortest possible time in order to maintain the thiocarbonylthio moieties during homogeneous aqueous RAFT polymerization.

Aqueous polymerizations were conducted at a constant CTA 1 to acrylamide (AM) ratio of 1/800 at pH 5.0. The ratio of CTA 1 to initiator 7 was maintained at 1.15 since higher ratios led to unacceptably low polymerization rate. Figure 2a shows the pseudo-first-order kinetic plots for the polymerization of acrylamide at 70 and 80 °C. At 90 °C with the above conditions, the polymerization was uncontrolled and the characteristic CTA color was lost immediately (data not shown), possibly due to hydrolysis. Only when the ratio of 1/7 was increased 5-fold was some degree of control attained. However, the first-order kinetic plot (Figure 2a, triangles) became increasingly nonlinear after 7.5 h. The molecular weight (obtained from SEC/MALLS) vs conversion plots for these aqueous polymerizations are shown in Figure 2b along with that theoretically predicted.

RAFT Polymerizations of Acrylamide in DMSO.

The aqueous polymerization data clearly demonstrate disparity between the experimental and theoretically predicted molecular weights and a loss of linear pseudo-first-order kinetic behavior at longer reaction times and higher temperatures. We therefore conducted polymerizations in DMSO to preclude competing CTA hydrolysis and thus allow extended polymerization times. CTAs 2 and 3 were chosen for study since they possess the same Z group as 1, are more soluble in DMSO, and have been used previously by our group for the RAFT polymerization of *N,N'*-dimethylacrylamide in organic solvents. Moreover, this allowed us to evaluate the effect of CTA structure and initiator half-life on the polymerization kinetics.

We first investigated the effect of increasing the initiator concentration at 70 °C maintaining a constant 800/1 acrylamide/CTA ratio. Figure 3a shows the anticipated increases in magnitude of the slopes of the

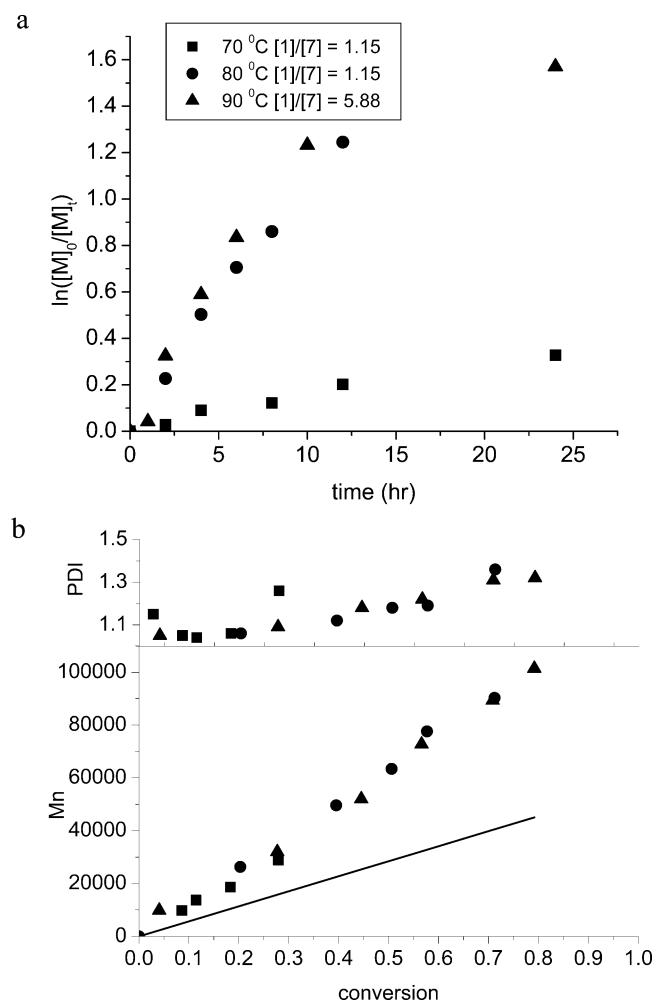


Figure 2. (a) Pseudo-first-order kinetic plot for the RAFT polymerization of acrylamide in aqueous buffer (pH = 5.0) using **1** as the CTA and **7** as the initiator at 70 °C, 80 °C ([**1**]/[**7**] = 1.15), and 90 °C ([**1**]/[**7**] = 5.88). (b) Molecular weight and PDI (obtained from SEC/MALLS) vs conversion plots for these aqueous polymerizations.

first-order rate plots as the initiator concentration increases relative to CTA. The M_n vs conversion plots (Figure 3b) are approximately linear in DMSO and water. However, experimentally measured values are higher than theoretically predicted at all conversions.

Another series of experiments utilizing CTAs **2** and **3** with stabilizing phenyl Z groups, but possessing different R groups, was carried out in DMSO at 70 °C. Kinetics of the polymerizations utilizing initiators **7** and **6** are shown in parts a and b of Figure 4, respectively.

CTA **2**, possessing the cumyl R group, often exhibits an induction period²⁶ as shown in Figure 4a with initiator **7**. However, when initiator **6** is utilized at a 5:1 ratio, no induction period is observed for the polymerization of acrylamide with either CTA **2** or **3**, and the initial slope is slightly greater with the latter. Figure 4b shows a dramatic loss in linear first-order behavior, with little or no conversion past 10 h (≈ 40 –45% total conversion) for the CTA/I ratio of 5/1. On the other hand, polymerization occurs rather smoothly (Figure 4a), obeying linear first-order kinetics up to 50 h for CTA **3** and 70 h for CTA **2** with a CTA:I ratio of 1.15. Parts a and b of Figure 4 illustrate the differences in kinetic profiles of acrylamide polymerization with CTAs **2** and **3** as dictated by initiators **6** and **7** with considerably different half-lives at 70 °C. For comparative purposes,

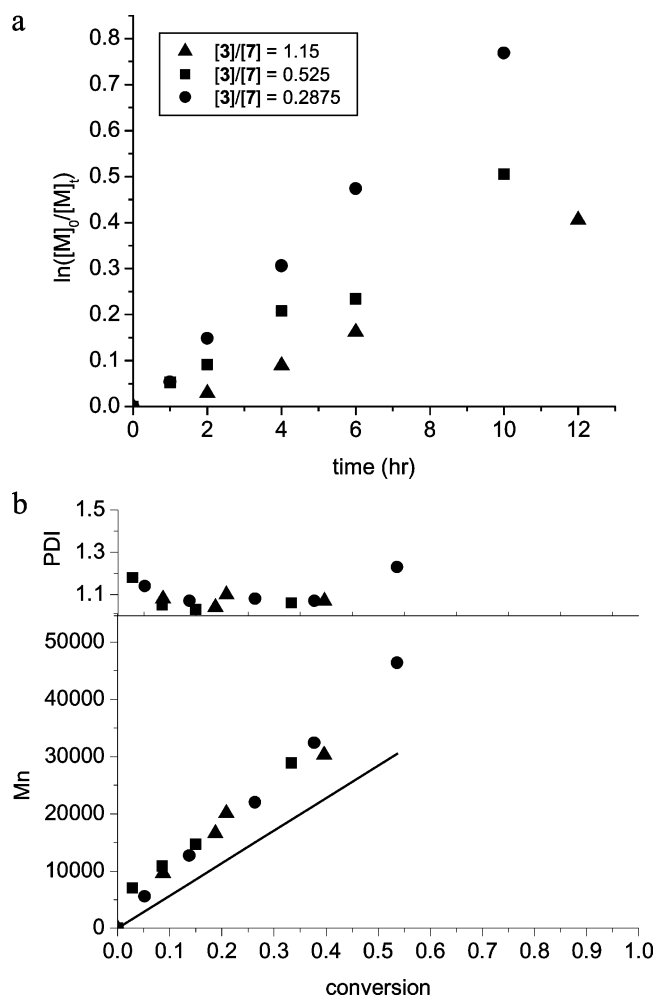


Figure 3. Pseudo-first-order kinetic plots for the effect of [CTA]:[I] ratio on the RAFT polymerization of acrylamide at 70 °C in DMSO with **3** as the CTA and **7** as the initiator. Monomer/CTA was maintained at 800/1. [CTA]/[I] ratios were 1.15 (\blacksquare), 0.575 (\bullet), and 0.2875 (\blacktriangle) and (b) M_n vs conversion plots for the [CTA]/[I] values shown in (a).

theoretical cumulative concentrations of initiator radicals (irrespective of their fate) vs time plots are shown in Figure 5c.

Rate enhancement and reduction/elimination of the induction period have often been demonstrated in RAFT polymerizations utilizing less stabilizing Z groups, for example benzyl vs phenyl.^{23,29,30,41} Therefore, we compared acrylamide polymerizations in DMSO at 70 °C utilizing CTAs **2** and **4** at a CTA/6 ratio of 5.0. Again, nonlinear kinetic profiles (Figure 6a) are observed as shown in the previous figure. Slower initial rates are observed with **2** as compared to **4**, as would be expected. M_n vs conversion curves (Figure 6b) have different slopes (and extrapolated y-intercept values) for the two CTAs. In both cases, considerable discrepancy remains between theoretical and experimental molecular weights; PDI values are higher with CTA **4**.

Results from the above studies suggested that, although it might be possible to extend conversion and enhance rate by proper initiator choice and/or increasing the initiator to CTA ratio, it would be more effective to substantially lower the activation energy for fragmentation of the intermediate **13**, provided selectivity of the propagating acrylamide species for the resulting macroCTA could be maintained. Therefore, the trithiocarbonate CTA **5** was employed for acrylamide polymeri-

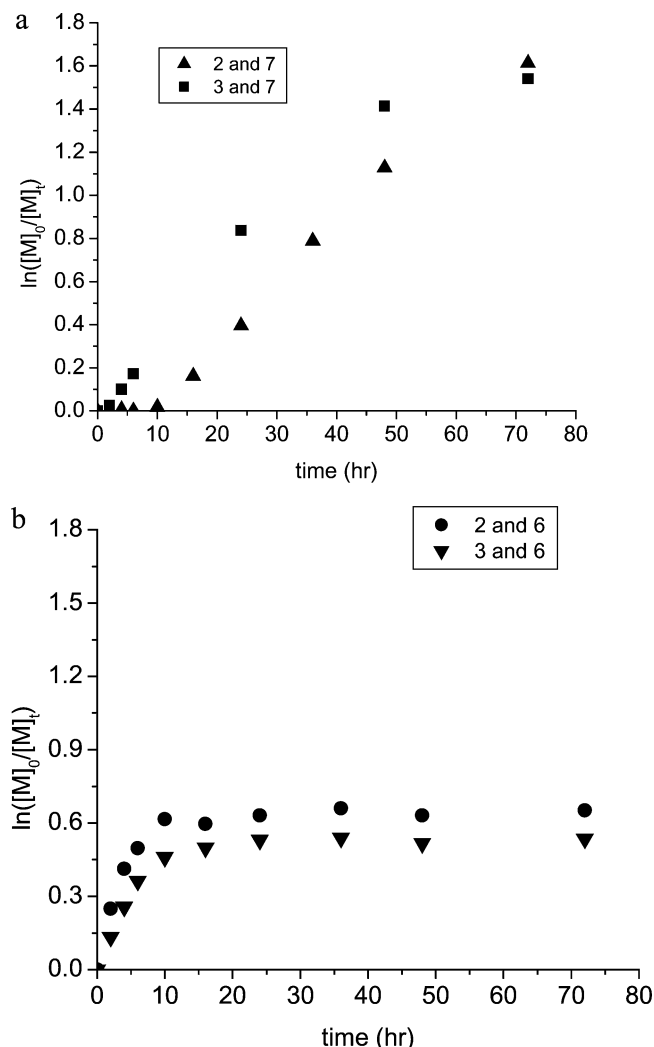


Figure 4. Kinetic plots for polymerization of acrylamide utilizing (a) initiator 6 and (b) initiator 7 with CTAs 2 and 3. [CTA]/[I] concentrations: ■, $[3]_0/[7]_0 = 1.15$; ●, $[3]_0/[6]_0 = 5.0$; ▲, $[2]_0/[7]_0 = 1.15$; ▼, $[2]_0/[6]_0 = 5.0$.

zation in DMSO at 70 °C. Figure 7a indicates the fastest rates of polymerization (8 times faster than with CTA 3, for example, under the same conditions) with approximately 75% conversion attained, well before the radical supply from initiator 6 is exhausted. Molecular weight and PDI vs conversion plots are shown in Figure 7b. Closer fits of theoretical and experimental molecular weights are obtained throughout the conversion range with PDIs well-controlled but increasing beyond 50% conversion.

Discussion

Kinetics of Acrylamide Polymerization. The inherent rate of monomer conversion during CTA-mediated RAFT polymerization is usually determined from the slope (equal to $k_p[P_n^*]$) of the first-order plot of $\ln([M]_0/[M]_t)$ vs time.^{31,33,34} For RAFT, the linear portion of the plot presumably occurs after attaining the main equilibrium (Scheme 1, step IV). Under RAFT conditions, intermediate radicals cannot add monomer, so the rate of monomer conversion is dependent on $[P_n^*]$. As in conventional polymerization, processes of radical generation, termination, and chain transfer can affect the concentration and reactivity of the propagating species and thus kinetic profiles.

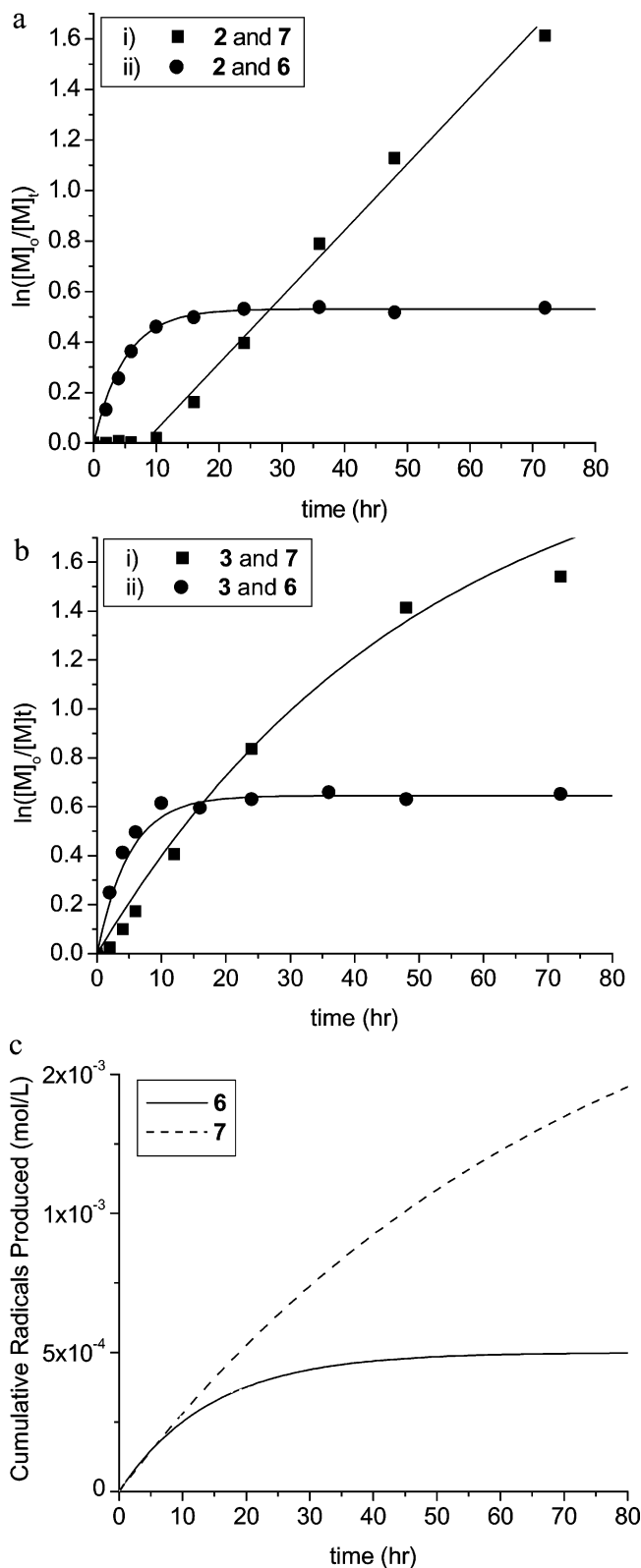


Figure 5. Pseudo-first-order kinetic plots of (a) 2- and (b) 3-mediated polymerization using 6 and 7 as the initiators. The shapes of the kinetic plots follow (c) the production of radicals as a function of time.

The CSIRO group in early RAFT studies³¹ clearly demonstrated that the rate of propagation after reaching step IV is related to steric and electronic factors operable during formation of the polymeric radical $[P_n^*]$ and to the ground-state stability of the intermediate 13. It should be noted that in our case the polyacrylamide

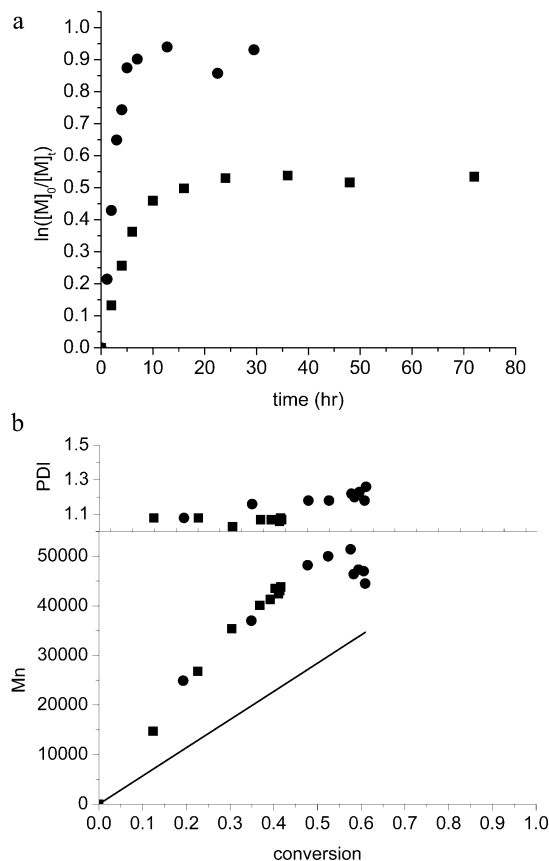
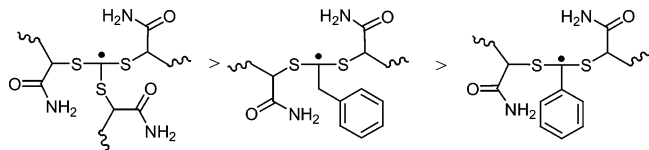


Figure 6. (a) Kinetics plots for acrylamide polymerizations in DMSO at 70 °C utilizing CTAs **2** (■) and **4** (●) at a CTA/initiator ratio of 5.0 and (b) M_n and PDI vs conversion plots.

radical is not an inherently good leaving group; though stabilized by the amide group, relatively weak steric effects (secondary carbon) and the strong P_n-S bond of **13** result in quite slow rates compared to many monomers. The CSIRO group also demonstrated experimentally that changes in the Z group greatly affect the fragmentation rate and thus the equilibrium concentration of propagating (nondormant) chains.³⁰ The nature of the propagating chain also determines selectivity toward macroCTA or monomer. Therefore, to control polymerization of acrylamide, which has an inherently high rate of propagation, relative rates of steps **III** (propagation) and **IV** (transfer) shown in Scheme 1 must be appropriately regulated.

As expected, values of the slopes from the first-order kinetic plots reflect the reactivity order of the respective intermediate radicals:



K^* ($k_p[P_n^*]$) values in Table 1 were determined early in the RAFT process but after sufficient time for achieving the “main” equilibrium (step IV, Scheme 1). By comparison, K^* (Table 1) in water or DMSO at 70 °C for initial acrylamide to CTA ratios of 800/1 increases from 1.3×10^{-2} to $5.0 \times 10^{-2} \text{ h}^{-1}$ with Z = phenyl (entries A, D, F, H–K, CTAs **1**, **2**, **3**) to $1.7 \times 10^{-1} \text{ h}^{-1}$ with Z = benzyl (entry L CTA **4**). The trithiocarbonate (entry M, CTA **5**) results in the highest value of $3.3 \times 10^{-1} \text{ h}^{-1}$.

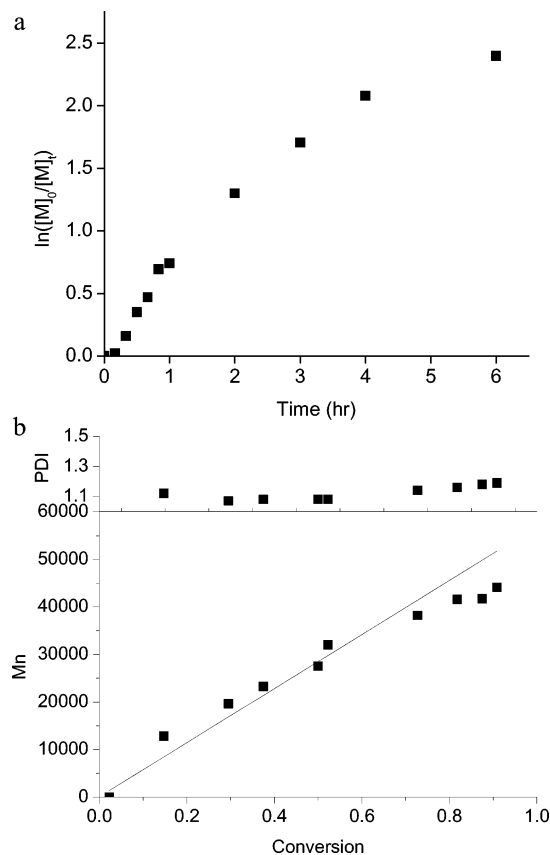


Figure 7. (a) Pseudo-first-order kinetic plot of the polymerization of acrylamide in DMSO mediated by CTA **5** and initiator **6** at 70 °C. (b) M_n and PDI vs conversion plots. $[5]/[6] = 5.0$.

The approximate 4- and 8-fold increases in $k_p[P_n^*]$ with CTAs **4** and **5**, respectively (entries L and M), as compared to CTAs **2** and **3** (entries J and K), are consistent with higher ground-state energies and lower fragmentation barriers of the respective symmetrical intermediates (**13**, Scheme 1).^{32,35–37} As expected, values of K^* increase with increasing temperature for a given Z group at the same CTA/initiator ratio.

The slopes of the linear first-order kinetic plots shown in Figure 3 (entries D, H, and I in Table 1) increase from 3.1×10^{-2} to 4.9×10^{-2} to $7.9 \times 10^{-2} \text{ h}^{-1}$ as the initiator concentration is increased at a constant acrylamide/CTA ratio of 800/1. These increasing slopes are expected and can be attributed to an increased number of active kinetic chains participating in the RAFT process.

In several of our previous studies of RAFT polymerization of acrylamido monomers in aqueous media,^{16,18} we noted substantial decreases in polymerization rate at long reaction times. This behavior was attributed to primary coupling reactions (**V**, Scheme 1) and should not be due to CTA hydrolysis since the latter would lead to reduced control and increasingly rapid monomer conversion.

The most prominent feature of the first-order kinetic plots of acrylamide polymerization in DMSO is the nonlinearity at longer times (Figures 4b and 5a,b). Complete cessation of polymerization is observed after 10 h with initiator **6** regardless of the nature of the mediating CTA (**2**, **3**, or **4**). The rather abrupt slope change in this case must be attributed to reduced numbers of active radicals participating in the main equilibrium (**IV**, Scheme 1) and/or to changes in the

Table 1. Kinetic and Molecular Weight Parameters for the Polymerization of Acrylamide

entry	CTA	solvent	I	[CTA] ₀ /[I] ₀	T (°C)	$K^* \times 10^2$ ^a (h ⁻¹)	t_{ind} (min) ^b	γ ^c	B ^d	r^2 values ^e
A	1	buffer	7	1.15	70	1.3 ± 0.1	0	0.59	2100	0.992
B	1	buffer	7	1.15	80	9.9 ± 0.5	0	0.43	0	0.993
C	1	buffer	7	5.88	90	15 ± 1	0			
D	3	DMSO	7	1.15	70	3.1 ± 0.2	30	0.81	4300	0.998
E	3	DMSO	7	5.88	90	9.9 ± 0.3	10	0.76	1400	0.989
F	2	DMSO	7	1.15	70	2.6 ± 0.2	500	0.77	7800	0.992
G	2	DMSO	7	5.88	90	2.7 ± 0.3	150	0.69	1800	0.990
H	3	DMSO	7	0.575	70	4.9 ± 0.5	10	0.83	3600	0.999
I	3	DMSO	7	0.288	70	7.9 ± 0.9	11	0.71	900	0.983
J	2	DMSO	6	5.00	70	4.0 ± 0.7	60	0.60	4300	0.987
K	3	DMSO	6	5.00	70	4.4 ± 0.8	0	0.65	0	0.979
L	4	DMSO	6	5.00	70	17 ± 6	0	0.77	12600	0.989
M	5	DMSO	6	5.00	70	33 ± 3	0	1.03	5000	0.999
N	5	DMSO	6	5.00	70	82 ± 5	0	1.28	6500	0.987
O	5	DMSO	6	5.00	70	33 ± 3	0	0.90	5900	0.999

^a Determined from the linear portion of the pseudo first-order kinetic plot. $K^* = k_p[P_n^*]$ where k_p is the rate constant for propagation and $[P_n^*]$ is the concentration of propagating radicals. ^b Determined from the x -intercept of the pseudo first-order kinetic plot. ^c Determined from the slope of the M_n vs conversion plot and eq 3. ^d Intercept values from eq 3. ^e Correlation coefficients for fit of γ and B values according to eq 3.

propagation rate coefficient. The shapes of the kinetic plots (Figure 6) arising from polymerizations with initiator **6** mediated by CTAs **2** and **4** are similar to those in Figure 4. Initially, monomer conversion is steady with a 4.3 times greater slope for **4** (entries J and L, Table 1); however, in the 8–10 h range slopes of the first-order kinetic plots rapidly decrease, and eventually monomer conversion rates become zero.

The differences in decomposition rates for initiators **6** and **7** allow for a qualitative examination of the relationship between the observed rates of polymerization and the radical supply during the RAFT process. Kinetic data for acrylamide polymerization mediated by **2** and **3** with initiators **6** and **7** are presented in Figure 5a,b for comparative purposes; here, the CTA concentrations are held constant relative to both initiators. Although **6** produces an enhanced rate of reaction initially with both CTAs **2** and **3**, the polymerization virtually stops after ~10 h or between 40% and 45% monomer conversion. Polymerizations with initiator **7** continue for 72 h, providing 79% and 80% monomer conversion. These results can be correlated with the respective time-dependent concentrations of radicals generated from the two initiators. In Figure 5c, the cumulative numbers of radicals produced from initiators **6** (solid line) and **7** (dashed line) are plotted vs time. The values were calculated from the respective initiator decomposition rate constants of 2.4×10^{-5} and $3.85 \times 10^{-6} \text{ s}^{-1}$, assuming an initiator efficiency of 0.5 at a temperature of 70 °C. Initiator **6** produces more radicals in the very early stages of reaction, resulting in higher rates of polymerization. After the first 10 h at 70 °C, however, the number of new radicals provided by **6** drops rapidly, while **7** continues to generate radicals for 72 h. Regardless of the specific fates of these radicals, the concentrations and predicted times to depletion of initiator-derived radical species correlate in a qualitative manner to the overall rates and eventual polymerization cessation.

One other feature of the plots in Figure 5a,b is noteworthy. Induction periods are often observed with CTAs in which R^* (Scheme 1) may reinitiate slowly^{28,32,36} or preferentially add back to CTA. Such an induction period, shown in Figure 4a for CTA **2** containing the cumyl leaving group, can be reduced or eliminated by choosing an initiator with a shorter half-life. Here, values of the induction period (t_{ind}) decreased from 500

to 30 min and 60 min to 0 min at 70 °C when **7** and **6**, respectively, were utilized as the initiators (Figure 5a,b). This would be anticipated on the basis of the elevated number of radicals produced in the preequilibrium steps of Scheme 1.

Molecular Weight Control in RAFT Polymerization of Acrylamide. The number-average molecular weight vs conversion curves, along with PDI vs conversion plots, for acrylamide polymerizations conducted with the CTAs **1–4** and initiators **6** and **7** are shown in Figures 2b, 3b, and 6b. In all cases, experimental M_n values are larger than those predicted by eq 1. If we follow the usual assumption that direct initiation is minimal, this equation may be rewritten as eq 2.

$$M_{n,\text{th}} = \frac{M_{\text{MW}}[M]_0\rho}{[\text{CTA}]_0} + \text{CTA}_{\text{MW}} \quad (2)$$

Furthermore, since the slopes of the molecular weight vs conversion plots are virtually linear for acrylamide polymerization mediated by CTAs **2–4** in DMSO with conversion, experimental data can be fit to (3), a modified form of eq 2.

$$M_{n,\text{th}} = \frac{M_{\text{MW}}[M]_0\rho}{[\text{CTA}]_0\gamma} + B \quad (3)$$

Here the simple parameter γ represents the extent of CTA utilization (efficiency) on a mole fraction basis over the measured conversion range for specified conditions; values of B represent an extrapolated intercept value, presumably due to monomer conversion (step III, Scheme 1) prior to the “main equilibrium”. These parameters, derived from linear fits of the experimental data, are listed in Table 1 and provide valuable information for targeting molecular weight based on initial CTA concentration under controllable conditions of RAFT synthesis. Obviously, values of γ near 1.0 and B approximating the molar mass of the CTA would reflect full utilization of the CTA early in the RAFT process.

A number of proposals have been put forward that suggest ways in which thiocarbonylthio groups are lost or stored during the RAFT process. The fate of intermediate species **10** and **13** (Scheme 1), their lifetimes, and concentrations as well as rates of fragmentation to R^* and P_n^* are subjects of intense debate.^{33,36–41,44–46}

However, our data clearly indicate that, regardless of mechanism, the number of participating dithioester groups has indeed been reduced, largely by a constant factor in both water and DMSO.

Greater discrepancies between observed and theoretical molecular weights for aqueous vs DMSO polymerizations are apparent in the respective molecular weight vs conversion plots and are reflected in the lower γ values in the former. For example, 70 °C data utilizing CTAs with the same Z group and with identical initiators and CTA/monomer ratios indicate an increase of γ from 0.59 in water (entry A, CTA **1**) to 0.77 (entry F, CTA **2**) and 0.81 (entry D, CTA **3**) in DMSO. A portion of the loss of CTA (or macroCTA) effectiveness is likely due to hydrolysis, even under the optimized pH 5 conditions we have recently reported for dithioester-mediated acrylamide polymerization.^{18,21} Clearly though, this contributes only to a part of molecular weight “overshoot”.

Comparisons of acrylamide polymerizations mediated by CTAs **2**, **3**, and **4** at 5/1 ratios with initiator **6** (entries J, K, and L) indicate increasing γ values of 0.60, 0.65, and 0.77, respectively. The first two CTAs would be expected to have similar but higher transfer coefficients when compared to the last since the phenyl Z group stabilizes intermediate **13** (Scheme 1) more effectively than the benzyl group.^{28,30,34} Thus, the activation energy for bond scission of **13** to yield active chain ends is lower for the benzyl Z group due to its higher ground-state energy as compared to the phenyl group.^{35,36} Since CTAs **2** and **4** have the same leaving groups and reinitiation efficiencies, it can be concluded that the greater fragmentation energy (longer lifetime at 70 °C) results in a lower γ value.

Polymerization of Acrylamide in the Presence of a Trithiocarbonate. Results from the acrylamide polymerization studies utilizing dithioesters **1** through **4** indicated that it is possible to increase the rates of polymerization, control molecular weight in a linear fashion with conversion, and maintain dithioester end groups for subsequent blocking. However, higher conversions and polymerization rates were desired. On the basis of literature reports of rapid conversions with xanthate and trithiocarbonate RAFT agents,^{8,30,47–50} we used CTA **5** for controlled polymerization under the same reaction conditions utilized with CTAs **2–4**. As expected, the less stabilized intermediate radicals (**13**, Scheme 1) afford much faster polymerization rates (Figure 7a, Table 1). The apparent rate of polymerization with **5** is highest of all the CTAs, approximately 8 times that mediated by **3**, as estimated from the slopes of the respective first-order kinetic plots. In approximately 4 h (Figure 7a), 74% of the monomer has reacted, long before the radical supply from **6** begins to diminish. Furthermore, the M_n vs conversion plots (Figure 7b) reveal the best agreement between observed and theoretical molecular weights utilizing CTA **5** with reaction conditions shown in Table 1. PDI values throughout the polymerization are quite low and in the controlled range, never getting above 1.2 (Figure 7b) at nearly complete monomer conversion.

Block Copolymer Synthesis Utilizing an Acrylamide MacroCTA. To demonstrate livingness, polyacrylamide macroCTAs prepared from CTAs **3** and **5** in DMSO were used to extend acrylamide and to prepare block copolymers with a variety of monomers. Results from that work⁵¹ will be presented in another paper to

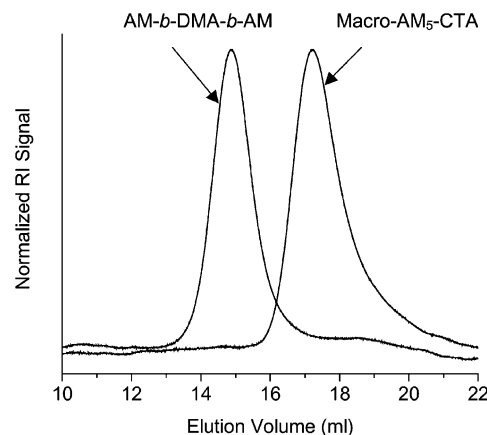


Figure 8. ASEC traces of the macroCTA and block copolymer prepared ($174\,000\text{ g mol}^{-1}$ and $M_w/M_n = 1.06$) using macro-AM₅-CTA ($M_n = 36\,200\text{ g mol}^{-1}$, $M_w/M_n = 1.25$) and DMA as the second monomer.

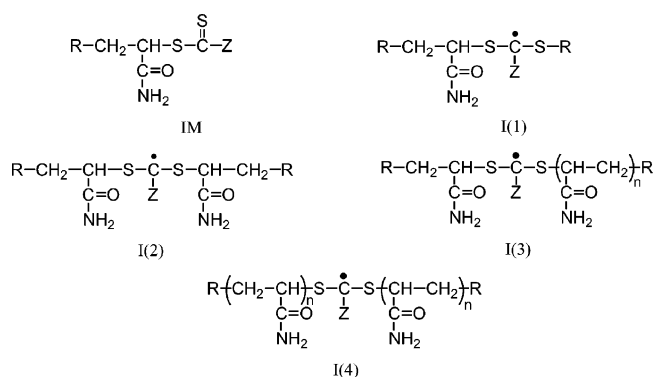


Figure 9. Initialized single monomer CTA IM and expected intermediates I(1)–I(4) produced during RAFT polymerization of acrylamide.

follow. We find that the trithiocarbonate macroCTA from **5** leads to best control. To illustrate, we present in Figure 8 the SEC traces of a polyacrylamide macroCTA from **5** of $36\,200\text{ g mol}^{-1}$ and PDI = 1.25 blocked with *N,N'*-dimethylacrylamide (DMA). As a consequence of the trithiocarbonate structure of this macroCTA, an ABA triblock copolymer, poly(AM-*b*-DMA-*b*-AM), is formed with a molecular weight of $174\,000\text{ g mol}^{-1}$ and PDI = 1.06. From the molecular weights of the macroCTA and the block copolymer, molar incorporation of the two monomers was determined as 29:71 (AM:DMA), which is in agreement with that determined by ¹H NMR spectroscopy.

Additional Considerations. After submission of our original manuscript, McLeary et al.⁴³ published results of an NMR spectroscopic investigation of the early kinetics of RAFT polymerization of styrene which may bring into focus the key issues regarding CTA-mediated control of polymerization rates and molecular weights. Although their CTA/monomer ratios were much higher than ours, an “initialization” period was identified during which the addition–fragmentation process is extremely selective toward formation of the single monomer adduct species from the initial RAFT agent. Accordingly in our work, species IM (Figure 9) would be formed from the starting CTA dithioester after addition of a single acrylamide monomer (step III, Scheme 1). Thus, reactions leading to the “main” equilibrium (step IV) would proceed through the intermediates I(1), I(2), I(3), and I(4) (Figure 9).

The asymmetric intermediate I(1) would preferentially fragment to the right since scission of the tertiary group is favored.^{28,36,50} Selectivity of various R groups for initialized CTA or monomer would determine the rate of formation of intermediate I(2), which might be expected to be the most stable (longest lifetime) radical of the four since fragmentation involves less sterically strained and relatively strong acrylamido unimer-to-sulfur bonds. Fragmentation of I(3) and I(4) should be progressively faster due to scission of oligomeric radicals as compared to unimeric species.^{36,50}

The relative rates of fragmentation of intermediates I(2), I(3), and I(4) and the related equilibrium constants for transfer determine the efficiency of the RAFT agent in the overall process and are greatly influenced by the Z group and reaction conditions including CTA/initiator concentration and temperature. Loss of efficiency from a slow transfer process (not all leaving groups from IM have reinitiated prior to step IV, Scheme 1) or from irreversible coupling of long-lived intermediate species would lead to higher than predicted molecular weights. The inhibition period at higher CTA/initiator ratios would also be expected from intermediate stabilizing Z groups.

Conclusions

The RAFT polymerization of acrylamide was investigated employing five CTAs and two initiators, at selected conditions. Higher rates of polymerization were achieved with CTAs having higher rates of fragmentation, initiators with lower decomposition temperatures, and higher initiator to CTA concentrations. High conversions, however, require a constant supply of initiator-derived radicals. The use of online light scattering, rather than standards, for the determination of molecular weight by SEC allows direct comparisons of experimental molecular weights with those predicted by theory. Molecular weight deviations for polymers prepared in water can be greater than those synthesized in DMSO. Adjustment of pH to values below 5.0 using appropriate buffers greatly diminishes hydrolysis and aminolysis of dithioesters; however, for increasingly extended reaction times (retarded rates), loss of macroCTA becomes an issue. Polymers produced under conditions of lower CTA to initiator concentrations exhibit greater deviations, while polymers prepared with CTAs with faster rates of fragmentation have molecular weights closer to those predicted by theory. Efficiency factors for CTA utilization were determined from linear fits of the experimental molecular weight vs conversion curves. A recent report by McLeary et al.⁴³ suggests that the polymerization behavior may be explained by species generated during "initialization" period during which the original CTA is converted to a single monomer RAFT species. Loss of efficiency may correlate with primary coupling of intermediate species I(1) or I(2) early in the RAFT process. The best control of conversion and molecular weight in the present study was obtained with CTA **5** and initiator **6** in DMSO (Table 1).

Acknowledgment. We gratefully acknowledge the financial support provided by GelTex Pharmaceuticals, Inc., the Department of Energy (DE-FC26-01BC15317), and the MRSEC program of the National Science Foundation (DMR-0213883).

References and Notes

- (1) Darling, T. R.; Davis, T. P.; Fryd, M.; Gridnev, A. A.; Haddleton, D. M.; Ittel, S. D.; Matheson, R. R.; Moad, G.; Rizzardo, E. *J. Polym. Sci., Polym. Chem.* **2000**, *38*, 1706–1708.
- (2) Wang, J. S.; Matyjaszewski, K. *J. Am. Chem. Soc.* **1995**, *117*, 5614–5615.
- (3) Kato, M.; Kamigaito, M.; Sawamoto, M.; Higashimura, T. *Macromolecules* **1995**, *28*, 1721–1723.
- (4) Georges, M. K.; Veregin, R. P. N.; Kazmaier, P. M.; Hamer, G. K. *Macromolecules* **1993**, *26*, 2987–2988.
- (5) Solomon, D. H.; Rizzardo, E. US Patent 4,581,429, 1986.
- (6) Quinn, J. F.; Davis, T. P.; Rizzardo, E. *Chem. Commun.* **2001**, 1044–1045.
- (7) Goto, A.; Sato, K.; Tsujii, Y.; Fukuda, T.; Moad, G.; Rizzardo, E.; Thang, S. H. *Macromolecules* **2001**, *34*, 402–408.
- (8) Chiefari, J.; Chong, Y. K.; Ercole, F.; Krstina, J.; Jeffery, J.; Le, T. P. T.; Mayadunne, R. T. A.; Meijs, G. F.; Moad, C. L.; Moad, G.; Rizzardo, E.; Thang, S. H. *Macromolecules* **1998**, *31*, 5559–5562.
- (9) Mitsukami, Y.; Donovan, M. S.; Lowe, A. B.; McCormick, C. L. *Macromolecules* **2001**, *34*, 2248–2256.
- (10) Shalaby, S. W.; McCormick, C. L.; Butler, G. B. In *ACS Symposium Series 467*; American Chemical Society: Washington, DC, 1991.
- (11) Sumerlin, B. S.; Donovan, M. S.; Mitsukami, Y.; Lowe, A. B.; McCormick, C. L. *Macromolecules* **2001**, *34*, 6561–6564.
- (12) Sumerlin, B. S.; Lowe, A. B.; Thomas, D. B.; McCormick, C. L. *Macromolecules* **2003**, *36*, 5982–5987.
- (13) Vasilieva, Y. A.; Thomas, D. B.; Scales, C. W.; McCormick, C. L. *Macromolecules* **2004**, *37*, 2728–2737.
- (14) Donovan, M. S.; Lowe, A. B.; Sanford, T. A.; McCormick, C. L. *J. Polym. Sci., Part A: Polym. Chem.* **2003**, *41*, 1262–1281.
- (15) Donovan, M. S.; Sumerlin, B. S.; Lowe, A. B.; McCormick, C. L. *Macromolecules* **2002**, *35*, 8663–8666.
- (16) Donovan, M. S.; Sanford, T. A.; Lowe, A. B.; Sumerlin, B. S.; Mitsukami, Y.; McCormick, C. L. *Macromolecules* **2002**, *35*, 4570–4572.
- (17) Donovan, M. S.; Lowe, A. B.; Sumerlin, B. S.; McCormick, C. L. *Macromolecules* **2002**, *35*, 4123–4132.
- (18) Thomas, D. B.; Sumerlin, B. S.; Lowe, A. B.; McCormick, C. L. *Macromolecules* **2003**, *36*, 1436–1439.
- (19) Convertine, A. J.; Ayres, N.; Scales, C. W.; Lowe, A. B.; McCormick, C. L.; *Biomacromolecules* **2004**, *5*, 1177–1180.
- (20) McCormick, C. L.; Lowe, A. B. *Acc. Chem. Res.* **2004**, *37*, 5, 312–325.
- (21) Thomas, D. B.; Convertine, A. J.; Hester, R. D.; Lowe, A. B.; McCormick, C. L. *Macromolecules* **2004**, *37*, 1735–1741.
- (22) Favier, A.; Charreyre, M.-T.; Chaumont, P.; Pichot, C. *Macromolecules* **2002**, *35*, 8271–8280.
- (23) Barner-Kowollik, C.; Quinn, J. F.; Nguyen, T. L. U.; Heuts, J. P. A.; Davis, T. P. *Macromolecules* **2001**, *34*, 7849–7857.
- (24) Prescott, S. W.; Ballard, M. J.; Rizzardo, E.; Gilbert, R. G. *Macromolecules* **2002**, *35*, 5417–5425.
- (25) Lai, J. T.; Filla, D.; Shea, R. *Macromolecules* **2002**, *35*, 6754–6756.
- (26) McCormick, C. L.; Donovan, M. S.; Lowe, A. B.; Sumerlin, B. S.; Thomas, D. B. Chain Transfer Agents for RAFT Polymerization in Aqueous Media. International Patent Application PCT/US03/02921 filed January 29, 2003.
- (27) Fevola, M. J.; Hester, R. D.; McCormick, C. L. *J. Polym. Sci., Part A: Polym. Chem.* **2003**, *41*, 560–568.
- (28) Chong, Y. K.; Krstina, J.; Le, T. P. T.; Moad, G.; Postma, A.; Rizzardo, E.; Thang, S. H. *Macromolecules* **2003**, *36*, 2256–2272.
- (29) Stenzel, M. H.; Cummins, L.; Roberts, E. G.; Davis, T. P.; Vana, P. *Macromol. Chem. Phys.* **2003**, *204*, 1160.
- (30) Chiefari, J.; Mayadunne, R. T. A.; Moad, C. L.; Moad, G.; Rizzardo, E.; Postma, A.; Skidmore, M. A.; Thang, S. H. *Macromolecules* **2003**, *36*, 2273–2283.
- (31) Moad, G.; Chiefari, J.; Chong, Y. K.; Krstina, J.; Mayadunne, R. T. A.; Postma, A.; Rizzardo, E.; Thang, S. H. *Polym. Int.* **2000**, *49*, 993–1001.
- (32) Vana, P.; Davis, T. P.; Barner-Kowollik, C. *Macromol. Theory Simul.* **2002**, *11*, 823–835.
- (33) Barner-Kowollik, C.; Coote, M. L.; Davis, T. P.; Radom, L.; Vana, P. *J. Polym. Sci., Polym. Chem.* **2003**, *41*, 2828–2832.
- (34) Schilli, C.; Lanzendöfer, M. G.; Müller, H. E. *Macromolecules* **2002**, *35*, 6819–6827.
- (35) Coote, M. L.; Radon, L. *J. Am. Chem. Soc.* **2003**, *125*, 1490–1491.

- (36) Coote, M. *Macromolecules* **2004**, *37*, 5023–5031.
- (37) Barner-Kowollik, C.; Quinn, J. F.; Morsley, D. R.; Davis, T. P. *J. Polym. Sci., Part A: Polym. Chem.* **2001**, *39*, 1353–1365.
- (38) Kwak, Y.; Goto, A.; Tsujii, Y.; Murata, Y.; Komatsu, K.; Fukuda, T. *Macromolecules* **2002**, *35*, 3026–3029.
- (39) Monteiro, M. J.; de Brouwer, H. *Macromolecules* **2001**, *34*, 349–352.
- (40) Wang, A. R.; Zhu, S.; Kwak, Y.; Goto, A.; Fukuda, T.; Monteiro, M. S. *J. Polym. Sci., Part A: Polym. Chem.* **2003**, *41*, 2833–2839.
- (41) Wang, A. R.; Zhu, S. *Macromol. Theory Simul.* **2003**, *12*, 663–668.
- (42) Chong, Y. K.; Le, T. P. T.; Moad, G.; Rizzardo, E.; Thang, S. H. *Macromolecules* **1999**, *32*, 2071–2074.
- (43) McCleary, J. B.; Calitz, F. M.; McKenzie, J. M.; Tonge, M. P.; Sanderson, R. D.; Klumperman, B. *Macromolecules* **2004**, *37*, 2383–2394.
- (44) Barner-Kowollik, C.; Vana, P.; Quinn, J. F.; Davis, T. P. *J. Polym. Sci., Part A: Polym. Chem.* **2002**, *40*, 1058–1063.
- (45) Toy, A. A.; Vana, P.; Davis, T. P.; Barner-Kowollik, C. *Macromolecules* **2004**, *37*, 744–751.
- (46) Kwak, Y.; Goto, A.; Komatsu, K.; Sugiura, Y.; Fukuda, T. *Macromolecules* **2004**, *37*, 4434–4440.
- (47) Destarac, M.; Charmot, D.; Franck, X.; Zard, S. Z. *Macromol. Rapid Commun.* **2000**, *21*, 1035–1039.
- (48) Adamy, M.; van Herk, A. M.; Destarac, M.; Monteiro, M. J. *Macromolecules* **2003**, *36*, 2293–2301.
- (49) Stenzel, M. H.; Cummins, Lyndal; Roberts, G. E.; Davis, T. P.; Vana, P.; Barner-Kowollik, C. *Macromol. Chem. Phys.* **2003**, *204*, 1160–1168.
- (50) Chong, Y. K.; Krstina, J.; Le, T. P. T.; Moad, G.; Postma, A.; Rizzardo, E.; Thang, S. H. *Macromolecules* **2003**, *36*, 2256–2272.
- (51) Thomas, D. B. Ph.D. Dissertation, University of Southern Mississippi, Dec 2003.

MA048199D